EUROPEAN ORGANIZATION FOR NUCLEAR RESEARCH

CERN-PPE/92-183

26 October 1992

Measurement of Inclusive Production of Light Meson Resonances in Hadronic Decays of the Z^0

DELPHI Collaboration

Abstract

A study of inclusive production of the meson resonances ϱ°, $K^{*\circ}(892)$, $f_o(975)$ and $f_2(1270)$ in hadronic decays of the Z^0 is presented. The measured mean meson multiplicity per hadronic event is 0.83 ± 0.14 for the ϱ°, 0.64 ± 0.24 for the $K^{*\circ}(892)$, 0.10 ± 0.04 for the $f_o(975)$ in the momentum range $p > 0.05 p_{beam}$ ($x_p > 0.05$) and 0.11 ± 0.05 for the $f_2(1270)$ for $x_p > 0.1$. These values and the corresponding differential cross sections $1/\sigma_{hadr} \cdot d\sigma/dx_p$ for the vector mesons are in good agreement with the predictions of the JETSET 7.3 PS and HERWIG 5.4 models. The $f_2(1270)$ production is overestimated by HERWIG but its x_p-shape is correctly reproduced. The measured ratios of the production cross sections $\sigma(f_2(1270))/\sigma(\varrho^0) = 0.22 \pm 0.08$ and $\sigma(f_2(1270))/\sigma(f_0(975)) = 3^{+7}_{-1}$ for $x_p > 0.1$ are consistent with the results obtained in hadronic reactions.

(Submitted to Physics Letters B)

P.Abreu[20], W.Adam[48], T.Adye[36], E.Agasi[30], G.D.Alekseev[14], A.Algeri[13], P.Allen[47], S.Almehed[23], S.J.Alvsvaag[4], U.Amaldi[7], E.G.Anassontzis[3], A.Andreazza[27], P.Antilogus[24], W-D.Apel[15], R.J.Apsimon[36], B.Åsman[43], J-E.Augustin[18], A.Augustinus[30], P.Baillon[7], P.Bambade[18], F.Barao[20], R.Barate[12], G.Barbiellini[45], D.Y.Bardin[14], G.Barker[33], A.Baroncelli[39], O.Barring[23], J.A.Barrio[25], W.Bartl[48], M.J.Bates[36], M.Battaglia[13], M.Baubillier[22], K-H.Becks[50], C.J.Beeston[33], M.Begalli[35], P.Beilliere[6], Yu.Belokopytov[41], P.Beltran[9], D.Benedic[8], A.C.Benvenuti[5], M.Berggren[18], D.Bertrand[2], F.Bianchi[44], M.S.Bilenky[14], P.Billoir[22], J.Bjarne[23], D.Bloch[8], S.Blyth[33], V.Bocci[37], P.N.Bogolubov[14], T.Bolognese[38], M.Bonesini[27], W.Bonivento[27], P.S.L.Booth[21], P.Borgeaud[38], G.Borisov[41], H.Borner[7], C.Bosio[39], B.Bostjancic[42], S.Bosworth[33], O.Botner[46], B.Bouquet[18], C.Bourdarios[18], T.J.V.Bowcock[21], M.Bozzo[11], S.Braibant[2], P.Branchini[39], K.D.Brand[34], R.A.Brenner[7], H.Briand[22], C.Bricman[2], R.C.A.Brown[7], N.Brummer[30], J-M.Brunet[6], L.Bugge[32], T.Buran[32], H.Burmeister[7], J.A.M.A.Buytaert[7], M.Caccia[7], M.Calvi[27], A.J.Camacho Rozas[40], R.Campion[21], T.Camporesi[7], V.Canale[37], F.Cao[2], F.Carena[7], L.Carroll[21], C.Caso[11], M.V.Castillo Gimenez[47], A.Cattai[7], F.R.Cavallo[5], L.Cerrito[37], V.Chabaud[7], A.Chan[1], M.Chapkin[41], Ph.Charpentier[7], L.Chaussard[18], J.Chauveau[22], P.Checchia[34], G.A.Chelkov[14], L.Chevalier[38], P.Chliapnikov[41], V.Chorowicz[22], J.T.M.Chrin[47], M.P.Clara[44], P.Collins[33], J.L.Contreras[25], R.Contri[11], E.Cortina[47], G.Cosme[18], F.Couchot[18], H.B.Crawley[1], D.Crennell[36], G.Crosetti[11], M.Crozon[6], J.Cuevas Maestro[40], S.Czellar[13], E.Dahl-Jensen[28], B.Dalmagne[18], M.Dam[32], G.Damgaard[28], G.Darbo[11], E.Daubie[2], A.Daum[15], P.D.Dauncey[33], M.Davenport[7], P.David[22], J.Davies[21], W.Da Silva[22], C.Defoix[6], D.Delikaris[7], S.Delorme[7], P.Delpierre[6], N.Demaria[44], A.De Angelis[45], H.De Boeck[2], W.De Boer[15], C.De Clercq[2], M.D.M.De Fez Laso[47], N.De Groot[30], C.De La Vaissiere[22], B.De Lotto[45], A.De Min[27], H.Dijkstra[7], L.Di Ciaccio[37], F.Djama[8], J.Dolbeau[6], M.Donszelmann[7], K.Doroba[49], M.Dracos[7], J.Drees[50], M.Dris[31], Y.Dufour[6], F.Dupont[12], L-O.Eek[46], P.A.-M.Eerola[7], R.Ehret[15], T.Ekelof[46], G.Ekspong[43], A.Elliot Peisert[34], J-P.Engel[8], N.Ershaidat[22], D.Fassouliotis[31], M.Feindt[7], M.Fernandez Alonso[40], A.Ferrer[47], T.A.Filippas[31], A.Firestone[1], H.Foeth[7], E.Fokitis[31], F.Fontanelli[11], K.A.J.Forbes[21], J-L.Fousset[26], S.Francon[24], B.Franek[36], P.Frenkiel[6], D.C.Fries[15], A.G.Frodesen[4], R.Fruhwirth[48], F.Fulda-Quenzer[18], K.Furnival[21], H.Furstenau[15], J.Fuster[7], G.Galeazzi[34], D.Gamba[44], C.Garcia[47], J.Garcia[40], C.Gaspar[7], U.Gasparini[34], Ph.Gavillet[7], E.N.Gazis[31], J-P.Gerber[8], P.Giacomelli[7], R.Gokieli[49], B.Golob[42], V.M.Golovatyuk[14], J.J.Gomez Y Cadenas[7], A.Goobar[43], G.Gopal[36], M.Gorski[49], V.Gracco[11], A.Grant[7], F.Grard[2], E.Graziani[39], G.Grosdidier[18], E.Gross[7], P.Grosse-Wiesmann[7], B.Grossetete[22], J.Guy[36], U.Haedinger[15], F.Hahn[50], M.Hahn[15], S.Haider[30], Z.Hajduk[16], A.Hakansson[23], A.Hallgren[46], K.Hamacher[50], G.Hamel De Monchenault[38], W.Hao[30], F.J.Harris[33], T.Henkes[7], J.J.Hernandez[47], P.Herquet[2], H.Herr[7], T.L.Hessing[21], I.Hietanen[13], C.O.Higgins[21], E.Higon[47], H.J.Hilke[7], S.D.Hodgson[33], T.Hofmokl[49], R.Holmes[1], S-O.Holmgren[43], D.Holthuizen[30], P.F.Honore[6], J.E.Hooper[28], M.Houlden[21], J.Hrubec[48], K.Huet[2], P.O.Hulth[43], K.Hultqvist[43], P.Ioannou[3], D.Isenhower[7], P-S.Iversen[4], J.N.Jackson[21], P.Jalocha[16], G.Jarlskog[23], P.Jarry[38], B.Jean-Marie[18], E.K.Johansson[43], D.Johnson[21], M.Jonker[7], L.Jonsson[23], P.Juillot[8], G.Kalkanis[3], G.Kalmus[36], F.Kapusta[22], M.Karlsson[7], E.Karvelas[9], S.Katsanevas[3], E.C.Katsoufis[31], R.Keranen[13], J.Kesteman[2], B.A.Khomenko[14], N.N.Khovanski[14], B.King[21], N.J.Kjaer[7], H.Klein[7], W.Klempt[7], A.Klovning[4], P.Kluit[30], A.Koch-Mehrin[50], J.H.Koehne[15], B.Koene[30], P.Kokkinias[9], M.Kopf[15], K.Korcyl[16], A.V.Korytov[14], V.Kostioukhine[41], C.Kourkoumelis[3], O.Kouznetsov[14], P.H.Kramer[50], J.Krolikowski[49], I.Kronkvist[23], U.Kruener-Marquis[50], W.Kucewicz[16], K.Kulka[46], K.Kurvinen[13], C.Lacasta[47], C.Lambropoulos[9], J.W.Lamsa[1], L.Lanceri[45], V.Lapin[41], J-P.Laugier[38], R.Lauhakangas[13], G.Leder[48], F.Ledroit[12], R.Leitner[29], Y.Lemoigne[38], J.Lemonne[2], G.Lenzen[50], V.Lepeltier[18], T.Lesiak[16], J.M.Levy[8], E.Lieb[50], D.Liko[48], J.Lindgren[13], R.Lindner[50], A.Lipniacka[49], I.Lippi[34], B.Loerstad[23], M.Lokajicek[14], J.G.Loken[33], A.Lopez-Fernandez[7], M.A.Lopez Aguera[40], M.Los[30], D.Loukas[9], J.J.Lozano[47], P.Lutz[6], L.Lyons[33], G.Maehlum[32], J.Maillard[6], A.Maltezos[9], F.Mandl[48], J.Marco[40], M.Margoni[34], J-C.Marin[7], A.Markou[9], T.Maron[50], S.Marti[47], L.Mathis[1], F.Matorras[40], C.Matteuzzi[27], G.Matthiae[37], M.Mazzucato[34], M.Mc Cubbin[21], R.Mc Kay[1], R.Mc Nulty[21], G.Meola[11], C.Meroni[27], W.T.Meyer[1], M.Michelotto[34], I.Mikulec[48], L.Mirabito[24], W.A.Mitaroff[48], G.V.Mitselmakher[14], U.Mjoernmark[23], T.Moa[43], R.Moeller[28], K.Moenig[7], M.R.Monge[11], P.Morettini[11], H.Mueller[15], W.J.Murray[36], G.Myatt[33], F.L.Navarria[5], P.Negri[27], B.S.Nielsen[28], B.Nijjhar[21], V.Nikolaenko[41], P.E.S.Nilsen[4], P.Niss[43], V.Obraztsov[41], A.G.Olshevski[14], R.Orava[13], A.Ostankov[41], K.Osterberg[13], A.Ouraou[38], M.Paganoni[27], R.Pain[22], H.Palka[30], Th.D.Papadopoulou[31], L.Pape[7], A.Passeri[39], M.Pegoraro[34], J.Pennanen[13], V.Perevozchikov[41], M.Pernicka[48], A.Perrotta[5], C.Petridou[45], A.Petrolini[11], T.E.Pettersen[34], F.Pierre[38], M.Pimenta[20], O.Pingot[2], S.Plaszczynski[18], M.E.Pol[7], G.Polok[16], P.Poropat[45], P.Privitera[15], A.Pullia[27], D.Radojicic[38], S.Ragazzi[27], H.Rahmani[31], P.N.Ratoff[19], A.L.Read[32], N.G.Redaelli[27], M.Regler[48], D.Reid[21], P.B.Renton[33], L.K.Resvanis[3], F.Richard[18], M.Richardson[21], J.Ridky[10], G.Rinaudo[44], I.Roditi[17], A.Romero[44], I.Roncagliolo[11], P.Ronchese[34], C.Ronnqvist[13], E.I.Rosenberg[1], S.Rossi[7], U.Rossi[5], E.Rosso[7], P.Roudeau[18], T.Rovelli[5], W.Ruckstuhl[30], V.Ruhlmann-Kleider[38], A.Ruiz[40], H.Saarikko[13], Y.Sacquin[38], G.Sajot[12], J.Salt[47], J.Sanchez[25], M.Sannino[11], S.Schael[15], H.Schneider[15], B.Schulze[37], M.A.E.Schyns[50], G.Sciolla[44], F.Scuri[45], A.M.Segar[33], R.Sekulin[36], M.Sessa[45], G.Sette[11], R.Seufert[15], R.C.Shellard[35], I.Siccama[30], P.Siegrist[38],

S.Simonetti[11], F.Simonetto[34], A.N.Sisakian[14], T.B.Skaali[32], G.Skjevling[32], G.Smadja[38,24], N.Smirnov[41], G.R.Smith[36], R.Sosnowski[7], T.S.Spassoff[12], E.Spiriti[39], S.Squarcia[11], H.Staeck[50], C.Stanescu[39], S.Stapnes[32], G.Stavropoulos[9], F.Stichelbaut[2], A.Stocchi[18], J.Strauss[48], J.Straver[7], R.Strub[8], M.Szczekowski[7], M.Szeptycka[49], P.Szymanski[49], T.Tabarelli[27], O.Tchikilev[41], G.E.Theodosiou[9], A.Tilquin[26], J.Timmermans[30], V.G.Timofeev[14], L.G.Tkatchev[14], T.Todorov[8], D.Z.Toet[30], O.Toker[13], A.Tomaradze[41], E.Torassa[44], L.Tortora[39], D.Treille[7], U.Trevisan[11], W.Trischuk[7], G.Tristram[6], C.Troncon[27], A.Tsirou[7], E.N.Tsyganov[14], M-L.Turluer[38], T.Tuuva[13], I.A.Tyapkin[22], M.Tyndel[36], S.Tzamarias[7], S.Ueberschaer[50], O.Ullaland[7], V.Uvarov[41], G.Valenti[5], E.Vallazza[44], J.A.Valls Ferrer[47], C.Vander Velde[2], G.W.Van Apeldoorn[30], P.Van Dam[30], M.Van Der Heijden[30], W.K.Van Doninck[2], P.Vaz[7], G.Vegni[27], L.Ventura[34], W.Venus[36], F.Verbeure[2], L.S.Vertogradov[14], D.Vilanova[38], P.Vincent[24], L.Vitale[13], E.Vlasov[41], A.S.Vodopyanov[14], M.Vollmer[50], G.Voulgaris[3], M.Voutilainen[13], V.Vrba[39], H.Wahlen[50], C.Walck[43], F.Waldner[45], M.Wayne[1], A.Wehr[50], M.Weierstall[50], P.Weilhammer[7], J.Werner[50], A.M.Wetherell[7], J.H.Wickens[2], J.Wikne[32], G.R.Wilkinson[33], W.S.C.Williams[33], M.Winter[8], M.Witek[16], D.Wormald[32], G.Wormser[18], K.Woschnagg[46], N.Yamdagni[43], P.Yepes[7], A.Zaitsev[41], A.Zalewska[16], P.Zalewski[18], D.Zavrtanik[42], E.Zevgolatakos[9], G.Zhang[50], N.I.Zimin[14], M.Zito[38], R.Zuberi[33], R.Zukanovich Funchal[6], G.Zumerle[34], J.Zuniga[47]

[1] Ames Laboratory and Department of Physics, Iowa State University, Ames IA 50011, USA
[2] Physics Department, Univ. Instelling Antwerpen, Universiteitsplein 1, B-2610 Wilrijk, Belgium
and IIHE, ULB-VUB, Pleinlaan 2, B-1050 Brussels, Belgium
and Faculté des Sciences, Univ. de l'Etat Mons, Av. Maistriau 19, B-7000 Mons, Belgium
[3] Physics Laboratory, University of Athens, Solonos Str. 104, GR-10680 Athens, Greece
[4] Department of Physics, University of Bergen, Allégaten 55, N-5007 Bergen, Norway
[5] Dipartimento di Fisica, Università di Bologna and INFN, Via Irnerio 46, I-40126 Bologna, Italy
[6] Collège de France, Lab. de Physique Corpusculaire, IN2P3-CNRS, F-75231 Paris Cedex 05, France
[7] CERN, CH-1211 Geneva 23, Switzerland
[8] Centre de Recherche Nucléaire, IN2P3 - CNRS/ULP - BP20, F-67037 Strasbourg Cedex, France
[9] Institute of Nuclear Physics, N.C.S.R. Demokritos, P.O. Box 60228, GR-15310 Athens, Greece
[10] FZU, Inst. of Physics of the C.A.S. High Energy Physics Division, Na Slovance 2, CS-180 40, Praha 8, Czechoslovakia
[11] Dipartimento di Fisica, Università di Genova and INFN, Via Dodecaneso 33, I-16146 Genova, Italy
[12] Institut des Sciences Nucléaires, IN2P3-CNRS, Université de Grenoble 1, F-38026 Grenoble, France
[13] Research Institute for High Energy Physics, SEFT, Siltavuorenpenger 20 C, SF-00170 Helsinki, Finland
[14] Joint Institute for Nuclear Research, Dubna, Head Post Office, P.O. Box 79, 101 000 Moscow, USSR.
[15] Institut für Experimentelle Kernphysik, Universität Karlsruhe, Postfach 6980, D-7500 Karlsruhe 1, FRG
[16] High Energy Physics Laboratory, Institute of Nuclear Physics, Ul. Kawiory 26 a, PL-30055 Krakow 30, Poland
[17] Centro Brasileiro de Pesquisas Físicas, rua Xavier Sigaud 150, RJ-22290 Rio de Janeiro, Brazil
[18] Université de Paris-Sud, Lab. de l'Accélérateur Linéaire, IN2P3-CNRS, Bat 200, F-91405 Orsay, France
[19] School of Physics and Materials, University of Lancaster - Lancaster LA1 4YB, UK
[20] LIP, IST, FOUL - Av. Elias Garcia, 14 - 1°, P-1000 Lisboa Codex, Portugal
[21] Department of Physics, University of Liverpool, P.O. Box 147, GB - Liverpool L69 3BX, UK
[22] LPNHE, IN2P3-CNRS, Universités Paris VI et VII, Tour 33 (RdC), 4 place Jussieu, F-75230 Paris Cedex 05, France
[23] Department of Physics, University of Lund, Sölvegatan 14, S-22363 Lund, Sweden
[24] Université Claude Bernard de Lyon, IPNL, IN2P3-CNRS, F-69622 Villeurbanne Cedex, France
[25] Universidad Complutense, Avda. Complutense s/n, E-28040 Madrid, Spain
[26] Univ. d'Aix - Marseille II - CPP, IN2P3-CNRS, F-13288 Marseille Cedex 09, France
[27] Dipartimento di Fisica, Università di Milano and INFN, Via Celoria 16, I-20133 Milan, Italy
[28] Niels Bohr Institute, Blegdamsvej 17, DK-2100 Copenhagen 0, Denmark
[29] NC, Nuclear Centre of MFF, Charles University, Areal MFF, V Holesovickach 2, CS-180 00, Praha 8, Czechoslovakia
[30] NIKHEF-H, Postbus 41882, NL-1009 DB Amsterdam, The Netherlands
[31] National Technical University, Physics Department, Zografou Campus, GR-15773 Athens, Greece
[32] Physics Department, University of Oslo, Blindern, N-1000 Oslo 3, Norway
[33] Nuclear Physics Laboratory, University of Oxford, Keble Road, GB - Oxford OX1 3RH, UK
[34] Dipartimento di Fisica, Università di Padova and INFN, Via Marzolo 8, I-35131 Padua, Italy
[35] Depto. de Fisica, Pontificia Univ. Católica, C.P. 38071 RJ-22453 Rio de Janeiro, Brazil
[36] Rutherford Appleton Laboratory, Chilton, GB - Didcot OX11 OQX, UK
[37] Dipartimento di Fisica, Università di Roma II and INFN, Tor Vergata, I-00173 Rome, Italy
[38] Centre d'Etude de Saclay, DSM/DAPNIA, F-91191 Gif-sur-Yvette Cedex, France
[39] Istituto Superiore di Sanità, Ist. Naz. di Fisica Nucl. (INFN), Viale Regina Elena 299, I-00161 Rome, Italy
[40] Facultad de Ciencias, Universidad de Santander, av. de los Castros, E - 39005 Santander, Spain
[41] Inst. for High Energy Physics, Serpukow P.O. Box 35, Protvino, (Moscow Region), CEI
[42] Institut "Jozef Stefan", Ljubljana, Slovenija
[43] Institute of Physics, University of Stockholm, Vanadisvägen 9, S-113 46 Stockholm, Sweden
[44] Dipartimento di Fisica Sperimentale, Università di Torino and INFN, Via P. Giuria 1, I-10125 Turin, Italy
[45] Dipartimento di Fisica, Università di Trieste and INFN, Via A. Valerio 2, I-34127 Trieste, Italy
and Istituto di Fisica, Università di Udine, I-33100 Udine, Italy
[46] Department of Radiation Sciences, University of Uppsala, P.O. Box 535, S-751 21 Uppsala, Sweden
[47] IFIC, Valencia-CSIC, and D.F.A.M.N., U. de Valencia, Avda. Dr. Moliner 50, E-46100 Burjassot (Valencia), Spain
[48] Institut für Hochenergiephysik, Österr. Akad. d. Wissensch., Nikolsdorfergasse 18, A-1050 Vienna, Austria
[49] Inst. Nuclear Studies and, University of Warsaw, Ul. Hoza 69, PL-00681 Warsaw, Poland
[50] Fachbereich Physik, University of Wuppertal, Postfach 100 127, D-5600 Wuppertal 1, FRG

1 Introduction

The production of the ϱ^0, $K^{*+}(892)$ and $K^{*0}(892)^\dagger$ vector mesons has been studied in many e^+e^- experiments [1 – 9] at energies below those presently available at LEP. Tensor meson and $f_0(975)$ production has been measured only in two of these experiments [4,5].

The measurement of the $K^{*+}(892)$ production using the DELPHI detector at LEP has been presented in ref.[10]. In this letter, measurements of the ϱ^0, $K^{*0}(892)$, $f_0(975)$ and $f_2(1270)$ production rates using the DELPHI detector are reported and comparison is made with other data and with predictions of the Monte Carlo generators JETSET 7.3 PS [11] and HERWIG 5.4 [12].

Both these programs implement a parton cascade based on perturbative QCD calculations, whereas the non-perturbative hadronization phase is described by phenomenological string and cluster fragmentation models, respectively. The programs have been used without the tensor meson contributions in JETSET and without the $f_0(975)$ contribution in both programs. The JETSET program has been used with default values of the ratio of s- to u-quarks and the ratio of pseudoscalar to vector mesons. Parameters related to global event shape were tuned as in [13]. The HERWIG program has been used with default values of parameters.

2 Event selection

This study is based on the sample of hadronic events collected with the DELPHI detector at the centre-of-mass energies around $\sqrt{s} = 91.2\ GeV$ in the 1991 running period of LEP. The DELPHI detector has been described in detail elsewhere [14]. Only charged particles reconstructed by the central detectors, including the microvertex, inner and outer detectors, forward chambers and the time projection chamber (TPC), are used in this analysis. A charged particle is required to satisfy the following criteria:

- momentum greater than 0.2 GeV/c,
- $\Delta p/p < 100\%$,
- polar angle between 25° and 155°,
- measured track length in the TPC greater than 50 cm and
- impact parameter with respect to the nominal crossing point within 5 cm in the transverse plane and 10 cm along the beam direction.

Events are accepted if

- there are at least 5 charged particles,
- the total energy of charged particles (assuming $\pi^\pm$ mass) in each of the two hemispheres with respect to the beam axis exceeds 3 GeV,
- the total energy of all charged particles is greater than 15 GeV and
- the polar angle θ of the sphericity axis is between 40° and 140°.

The resulting data sample comprised 191,796 events. The contamination from events due to beam-gas scattering, $\gamma\gamma$ interactions and $\tau^+\tau^-$ events is estimated to be less than 0.3% of the selected events. To ensure that the analysis is restricted to charged particles originating from, or close to, the primary vertex, invariant masses of particle pairs are calculated for particles with the impact parameter relative to the reconstructed event vertex, within 0.3 cm in the transverse plane and 2 cm along the beam direction.

[†] In the following the charge conjugate states for $K^{*+}(892)$, $K^{**}(892)$, $K_2^{*+}(1430)$ and $K_2^{**}(1430)$ are always assumed.

3 Method of analysis

A well known difficulty in resonance studies arises when particle identification efficiency is low and each particle is assigned a pion or kaon mass depending on the invariant-mass distribution ($\pi^+\pi^-$ or $K^\pm\pi^\mp$) under study. This leads not only to an increased combinatorial background (which is already large due to the large number of secondaries at high energies), but also to the problem of "reflections" when the resonance signals in a particular particle combination (e.g. $K^+\pi^-$) distort the invariant-mass spectrum of other combinations (e.g. $\pi^+\pi^-$) due to a particle (e.g. K^+) being wrongly identified (e.g. as a π^+). These reflections are particularly severe when (narrow) resonances overlap in phase space.

The fitting procedure applied to the invariant-mass distributions to extract resonance cross sections and, in particular, the treatment of reflections due to particle misidentification used in this study are very similar to those described in ref.[15,16]. The $\pi^+\pi^-$ and $K^\pm\pi^\mp$ invariant-mass distributions in the total available range of $x_p(= p/p_{beam})$, as well as in each x_p-interval are fitted with the expressions:

$$d\sigma/dM_{\pi\pi} = \beta_{K^\circ} BW_{K^\circ} + BG_{\pi\pi}(\alpha_{\pi\pi} + \beta_{\varrho^\circ} BW_{\varrho^\circ} + \beta_{f_\circ} BW_{f_\circ} + \beta_{f_2} BW_{f_2}), \quad (1)$$

$$d\sigma/dM_{K\pi} = BG_{K\pi}(\alpha_{K\pi} + \beta_{K^*} BW_{K^*} + \beta_{K_2^*} BW_{K_2^*}), \quad (2)$$

where α and β are fitted parameters and BW is a Breit-Wigner function with two free parameters: the central mass $M_\circ$ and total width Γ, assumed to be a sum of the natural width $\Gamma_\circ$ and the experimental resolution width Γ_R (for a justification, see for example [16]). A relativistic P-wave BW function is used for the ϱ° and $K^{*\circ}(892)$, an S-wave function for the $f_\circ(975)$ and a D-wave function for the $f_2(1270)$ and $K_2^{*\circ}(1430)$. A narrow peak near $500 MeV/c^2$ in the $\pi^+\pi^-$ invariant mass spectrum corresponding to the $K_S^\circ \to \pi^+\pi^-$ decay is described by non-relativistic BW function. The function used for the background BG is

$$BG = (M - M_{th})^{\gamma_1} exp(\gamma_2 M + \gamma_3 M^2 + \gamma_4 M^3 + \gamma_5 M^4). \quad (3)$$

For the $\pi^+\pi^-$ invariant mass distributions for $0.1 < x_p < 0.4$, fitted between 0.44 and 2.3 GeV/c^2, all the five $\gamma's$ are free parameters in the fit. For the higher and lower x_p ranges the $\pi^+\pi^-$ mass distribution is fitted only between 0.44 and 1.3 GeV/c^2, so γ_4 and γ_5 are fixed to zero. These two parameters are also fixed to zero for the $K^\pm\pi^\mp$ mass distributions, fitted between 0.76 and 1.64 GeV/c^2 for all x_p ranges. M_{th} is the threshold mass for the relevant mass combination. Other forms of background parametrization have also been tried and give the same results within errors.

Besides (1)–(2), the data have also been fitted by the expressions:

$$d\sigma/dM_{\pi\pi} = \alpha_{\pi\pi} BG_{\pi\pi} + \beta_{K^\circ} BW_{K^\circ} + \beta_{\varrho^\circ} BW_{\varrho^\circ} + \beta_{f_\circ} BW_{f_\circ} + \beta_{f_2} BW_{f_2}, \quad (4)$$

$$d\sigma/dM_{K\pi} = \alpha_{K\pi} BG_{K\pi} + \beta_{K^*} BW_{K^*} + \beta_{K_2^*} BW_{K_2^*}, \quad (5)$$

i.e. by a sum of BW functions and the background function BG of (3). The results obtained are the same within errors.

The reflections have been treated in the following way. Each $\pi^+\pi^-$ combination is weighted by the product of $W_{K^+\pi^-}$ and $W_{\pi^+K^-}$ which are the probabilities that the combination does not belong to the $K^{*0}(892)$ or $K^{*0}(1430)$ or to the $\overline{K}^{*0}(892)$ and $\overline{K}^{*0}(1430)$. Similarly, for each $K^+\pi^-$ pair the weights $W_{\pi^+K^-}$ and $W_{\pi^+\pi^-}$ (and for π^+K^- pair weights

$W_{K^+\pi^-}$ and $W_{\pi^+\pi^-}$) account for the effects of resonances in the π^+K^- and $\pi^+\pi^-$ (in $K^+\pi^-$ and $\pi^+\pi^-$) invariant-mass distributions. The weights are defined as

$$W_{\pi\pi} = \frac{\alpha_{\pi\pi} BG_{\pi\pi}}{\beta_{K^\circ} BW_{K^\circ} + BG_{\pi\pi}(\alpha_{\pi\pi} + \beta_{\varrho^\circ} BW_{\varrho^\circ} + \beta_{f_\circ} BW_{f_\circ} + \beta_{f_2} BW_{f_2})}, \tag{6}$$

$$W_{K\pi} = \frac{\alpha_{K\pi}}{\alpha_{K\pi} + \beta_{K^*} BW_{K^*} + \beta_{K_2^*} BW_{K_2^*}}. \tag{7}$$

The expression for the weight $W_{\pi^+K^-}$ is the same as $W_{K^+\pi^-}$ since the $K^\pm\pi^\mp$ invariant mass spectrum is fitted, but it is calculated for the mass $M_{\pi^+K^-}$ (for the same particle pair).

The procedure is iterative and consists of the following two steps for the i-th iteration:

- the $\pi^+\pi^-$ invariant-mass spectrum is calculated using the product of the weights $W_{K\pi}(i-1) \cdot W_{\pi K}(i-1)$. The cross sections for the ϱ°, $f_\circ(975)$, $f_2(1270)$ and for the peak related to the $K^\circ_S \to \pi^+\pi^-$ decay are determined from the fit, together with weights $W_{\pi\pi}(i)$;
- the $K^\pm\pi^\mp$ invariant-mass spectrum is calculated using the weights $W_{\pi\pi}(i) \cdot W_{\pi K}(i-1)$ (for $K^+\pi^-$ pairs) and $W_{\pi\pi}(i) \cdot W_{K\pi}(i-1)$ (for π^+K^- pairs) and the $K^{*\circ}(892)$, $K_2^{*\circ}(1430)$ cross sections and the weights $W_{K\pi}(i)$ and $W_{\pi K}(i)$ are determined.

For the first iteration all weights $W(0)$ are equal to 1.

To obtain the differential cross sections, $1/\sigma_{hadr} \cdot d\sigma/dx_p$, this procedure has been applied to each x_p-interval. It converges fairly quickly, three iterations being sufficient in all cases considered. This procedure has been checked with events generated by JETSET 7.3 PS and HERWIG 5.4, with the input values of the resonance cross sections adjusted to the experimental values. Consistent results are obtained. It has also been checked, using generated events, that the reflections from the ω, ϕ, η and η' do not influence the results.

The raw $\pi^+\pi^-$ and $K^\pm\pi^\mp$ invariant mass distributions and those corrected for reflections are shown in figs. 1–2 respectively. The values of $M_\circ$ and Γ obtained from the fits are given in table 1. The central mass values $M_\circ$ are consistent with the world average values from the PDG tables [17]; while the values for Γ are somewhat larger than the world average values. The difference indicates the size of the mass resolution (Γ_R) consistent with the value of Γ_R determined from the track error matrices. The final results, shown in figs. $1-2$, are therefore obtained with fits performed with the total widths fixed at $\Gamma = \Gamma_{PDG} + \Gamma_R$. The invariant mass distributions exhibit clear ϱ°, $f_\circ(975)$ and $f_2(1270)$ signals, the peak related to the $K^\circ_S \to \pi^+\pi^-$ decay (fig. 1), $K^{*\circ}(892)$ and $K^{*\circ}(1430)$ signals (fig. 2). However, at the present level of statistics and without using particle identification the $K^{*\circ}(1430)$ cross section cannot be reliably determined.

The resonance cross sections are determined by integrating the Breit-Wigner functions obtained in the fits with expressions (4), (5) or as

$$\sigma = \beta \int BW(M)BG(M)dM, \tag{8}$$

when expressions (1) and (2) have been used. The Monte Carlo program DELSIM [18] is used to correct the extracted cross sections for geometrical acceptance, kinematical cuts, particle interactions within the detector material and other detector imperfections. Events were generated using JETSET 7.2 PS program with default parameters. The particles were followed through each detector and simulated digitizations obtained processed with the same reconstruction and analysis programs as the experimental data.

The invariant mass distributions from the simulated events are in good agreement with the data. This is illustrated in fig. 2, where the $K^\pm\pi^\mp$ mass spectrum for the simulated

events is compared with the real distribution. It should be noted that the normalization is done to the total number of hadronic events and not specifically to the number of the entries in the invariant mass distributions. The observed difference in the normalisation is therefore due to small differences in the averaged charged multiplicity in simulated and real data events. Still, the simulated events reproduce the data with an accuracy better than 6% in the fitted mass regions. The disagreement is larger in the low mass region. The observed resolution in the resonance mass regions is consistent with expectations from Monte Carlo simulation.

The efficiency for vector mesons is obtained by comparing their cross sections in JETSET with the ones determined from the simulated events applying the same fitting procedure as for the data. For the $f_0(975)$ and $f_2(1270)$, not generated by the JETSET, the same efficiency as for ρ^0 has been assumed, but corrected for different values of $C(M) = (d\sigma/dM)_J/(d\sigma/dM)_D$ in the ρ^0, $f_0(975)$ and $f_2(1270)$ mass regions, where $(d\sigma/dM)_J$ and $(d\sigma/dM)_D$ are invariant-mass spectra obtained using JETSET and, respectively, the generated events passed through the detector simulation and reconstruction programs. The efficiencies obtained in this way are given in table 1.

The systematic errors are dominated by uncertainties in the efficiency determination due to limited statistics of 60 000 generated events. They are given as the second error in table 2 and combined quadratically with the statistical errors for the data points in fig. 3 (see below). However these errors are not taken into account in the $1/\sigma_{hadr} \cdot d\sigma/dx_p$ differential cross sections,[‡] nor in the $\sigma(\rho^0)/\sigma(f_2(1270))$ and $\sigma(f_2(1270))/\sigma(f_0(975))$ ratios. Systematic uncertainties arising from the fitting procedure, such as choice of background shape, fitting expression, fit range and the assumed resolution, are taken into account. The results presented are corrected for unobserved resonance decay modes.

4 Results

The measured average multiplicities per hadronic event of the ϱ°, $K^{*\circ}(892)$, $f_0(975)$ and $f_2(1270)$ in the x_p-ranges indicated (given in table 2) are obtained by normalisation of the determined resonance cross sections to the total hadronic cross section σ_{hadr}. For the vector mesons, they are in good agreement with the JETSET 7.3 PS and HERWIG 5.4 predictions also presented in table 2. The mean multiplicities of the ϱ° and $K^{*\circ}(892)$ resonances, for the full $x_p > 0$ range are obtained from the measured ones for $x_p > 0.05$ by extrapolation, assuming the x_p-shape predicted by JETSET. Uncertainties in the extrapolation are estimated by comparing the x_p-shapes predicted by JETSET and HERWIG and are included in the errors.

Our results for ϱ° and $K^{*\circ}(892)$ for $x_p > 0$ are compared with other e^+e^- data [1 – 10] at different centre-of-mass energies[§] and with the energy dependence predicted by JETSET and HERWIG in fig. 3. The rise of resonance production with increasing energy is noticeably slower in HERWIG than in JETSET, especially for the ϱ°, where the disagreement between the low energy data and HERWIG is quite significant. Fig. 3 also indicates that the difference between JETSET and HERWIG will increase at higher LEP energies.

The measured ratio

$$\sigma(f_2(1270))/\sigma(\varrho^\circ) = 0.22 \pm 0.08 \qquad (9)$$

[‡]The average resonance multiplicities obtained by integrating of the x_p-spectra are in very good agreement with the ones obtained for the full x_p-ranges.

[§]In all these experiments the average resonance multiplicities have also been measured in the restricted x_p-ranges and then extrapolated to the $x_p > 0$ region assuming the x_p-shape predicted by the models.

for $x_p > 0.1$ can be compared with the tensor-to-vector meson ratios in the full x_p-range measured in hadronic reactions: $\sigma(K_2^{*+}(1430))/\sigma(K^{*+}(892)) = 0.25 \pm 0.04$ [19], $\sigma(K_2^{*\circ}(1430))/\sigma(K^{*\circ}(892)) = 0.23 \pm 0.08$, $\sigma(f_2(1270))/\sigma(\varrho^\circ) = 0.26 \pm 0.05$ [20], 0.30 ± 0.06 [15] and 0.24 ± 0.03 [21] (with an average value of 0.25 ± 0.03) in the beam momentum range between 32 and 400 GeV/c. Our result agrees within errors with these values.

The measured ratio

$$\sigma(f_2(1270))/\sigma(f_\circ(975)) = 3^{+7}_{-1} \tag{10}$$

for $x_p > 0.1$ can be compared with the corresponding values of 2 ± 1 in e^+e^- annihilation at 29 *GeV* [5] and 4.1 ± 1.5 in pp-interactions at $\sqrt{s} = 27.5$ *GeV* [21]. It is of interest that all these results are consistent, within large errors, with the simple spin statistics prediction of 5 for the ratio of the tensor-to-scalar mesons.

The differential cross sections, $1/\sigma_{hadr} \cdot d\sigma/dx_p$, for the ϱ°, $f_2(1270)$, $f_\circ(975)$ and $K^{*\circ}(892)$ are shown in fig. 4, together with the JETSET and HERWIG predictions for vector mesons and the HERWIG prediction for the $f_2(1270)$. The agreement between data and models for vector mesons is quite impressive. The shape of the $f_2(1270)$ x_p-spectrum, consistent with the HERWIG prediction, is similar to that of the $f_\circ(975)$.

5 Summary and conclusions

The inclusive production of light meson resonances has been analysed from a sample of about 200 000 hadronic Z^0 decays collected by the DELPHI detector from 1991 LEP running period.

The average multiplicities and x_p-spectra of ϱ°, $K^{*\circ}(892)$, $f_\circ(975)$ and $f_2(1270)$ mesons have been measured. For the vector mesons, ϱ° and $K^{*\circ}(892)$, good agreement is found between data and JETSET 7.3 PS and HERWIG 5.4 models.

The production cross section ratio between $f_2(1270)$ and ϱ° is found to be 0.22 ± 0.08 which agrees with the tensor-to-vector meson ratio of 0.25 ± 0.03 measured in hadronic reactions. The production cross section ratio between $f_2(1270)$ and $f_\circ(975)$, found to be 3^{+7}_{-1}, is consistent, within large errors, with the measurements in two other experiments and with the simple spin statistics prediction. HERWIG overestimates the $f_2(1270)$ production rate, but reproduces the shape of its x_p-spectrum.

Our measurement of the $f_2(1270)$ production together with results of other experiments shows that tensor meson production rate is not negligible and should be taken into account in the JETSET model. To a smaller extent this is also true for $f_\circ(975)$, which is neglected both in JETSET and HERWIG.

After this work was completed we became aware of the OPAL results on the $K^{*\circ}(892)$ production[22]. Their value of the average $K^{*\circ}(892)$ multiplicity, $0.76 \pm 0.07 \pm 0.06$, agrees within errors with our result.

Acknowledgements

We are greatly indebted to our technical collaborators and to the funding agencies for their support in building and operating the DELPHI detector, and to the members of the CERN-SL Division for the excellent performance of the LEP collider. We thank B.Webber for interesting discussions.

References

[1] TASSO Collaboration, W.Brandelik et al., Phys. Lett. **B117** (1982) 135.

[2] JADE Collaboration, W.Bartel et al., Phys. Lett. **B145** (1984) 441.

[3] TPC Collaboration, H.Aihara et al., Phys. Rev. Lett. **53** (1984) 2378;
T.K.Edberg, Ph.D. Thesis "Inclusive Production of Vector Mesons in e^+e^- Annihilation at $\sqrt{s} = 29GeV$", LBL-25652 (1988).

[4] CLEO Collaboration, S.Behrends et al., Phys. Rev. **31** (1985) 2161.

[5] HRS Collaboration, S.Abachi et al., Phys. Rev. Lett. **57** (1986) 1990; Phys. Lett. **B199** (1987) 151.

[6] HRS Collaboration, S.Abachi et al., Phys. Rev. **D40** (1989) 706.

[7] TASSO Collaboration, W.Braunschweig et al., Z.Phys. **C47** (1990) 167.

[8] CELLO Collaboration, H.-J. Behrend et al., Z.Phys. **C46** (1990) 397.

[9] ARGUS Collaboration, A.Albrecht et al., Z.Phys. **C41** (1989) 557;
A.Lindner, "Messung der $K^*(892)$-, ρ^0-, ω- und $f_0(975)$- Produktion in Ereignissen der e^+e^--Annihilation bei Energien im Bereich der Υ-Resonanzen", Dissertation von Diplom-Physiker, Dortmund, February 1992.

[10] DELPHI Collaboration, P.Abreu et al., Phys. Lett. **B275** (1992) 231.

[11] JETSET Monte Carlo Program:
T.Sjöstrand, Comp. Phys. Commun. **39** (1986) 347,
T.Sjöstrand and M.Bengtsson, Comp. Phys. Commun. **43** (1987) 367.

[12] HERWIG Monte Carlo Program:
G.Marchesini and B.Webber, Nucl.Phys. **B310** (1988) 461,
I.G.Knowels, Nucl.Phys. **B310** (1988) 571,
G.Marchesini et al., Comp. Phys. Commun. **67** (1992) 465.

[13] DELPHI Collaboration, "Comparison of data with QCD models", contributed paper to the LP-EPS conference, Geneva, August 1991.

[14] DELPHI Collaboration, P.Aarnio et al., Nucl. Instr. and Meth. **A303** (1991) 233.

[15] NA22-EHS Collaboration, N.M.Agababyan et al., Z.Phys. **C41** (1989) 539.

[16] ABBCCHW Collaboration, M.Deutschmann et al., Nucl. Phys. **B103** (1976) 426.
Mirabelle Collaboration, P.Granet et al., Nucl. Phys. **B140** (1978) 389.

[17] PDG, K.Hikasa et al., Phys. Rev. **D45** (1992) 1.

[18] DELSIM User Guide, **DELPHI 87-96 PROG-99**, Geneva, July 1989;
DELSIM Reference Manual, **DELPHI 87-98 PROG-100**, Geneva, July 1989.

[19] Mirabelle Collaboration, I.V.Ajinenko et al., Z.Phys. **C24** (1984) 103.

[20] Mirabelle Collaboration, P.V.Chliapnikov et al., Nucl. Phys. **B176** (1980) 303; Z.Phys. **C12** (1982) 113.

[21] NA27 (LEBC-EHS) Collaboration, M.Aguilar-Benitez et al., Z.Phys. **C50** (1991) 405.

[22] OPAL Collaboration, P.D.Acton et al., Inclusive Neutral Vector Meson Production in Hadronic Z^0 Decays, CERN-PPE/92-116(1992).

Table 1

The efficiency in determination of resonance cross section, resonance central mass M_o, total width Γ (with a contribution from the mass resolution) and mass resolution obtained in the indicated x_p-range using the procedures described in the text.

Resonance	x_p-range	$Efficiency(\%)$	$M_o(MeV/c^2)$	$\Gamma(MeV/c^2)$	$\Gamma_R(MeV/c^2)$
ϱ°	$x_p > 0.05$	42±6	757±2	151±11	11
$K^{*\circ}(892)$	$x_p > 0.05$	32±10	890±2	55±5	6
$f_o(975)$	$x_p > 0.05$	40±7	961±4	64±17	14
$f_2(1270)$	$x_p > 0.1$	32±7	1293±13	185±57	21

Table 2

Average multiplicity of resonances per hadronic event in indicated x_p-ranges in comparison with the JETSET 7.3 PS and HERWIG 5.4 predictions.

		Average resonance multiplicity		
Resonance	x_p-range	Experiment	JETSET 7.3 PS	HERWIG 5.4
ϱ°	$x_p > 0.1$	0.51 ±0.05 ±0.09	0.54	0.51
	$x_p > 0.05$	0.83 ±0.07 ±0.12	0.90	0.85
	$x_p > 0$	1.43 ±0.12 ±0.22 [1)]	1.55	1.40
$K^{*\circ}(892)$	$x_p > 0.1$	0.36 ±0.09 ±0.13	0.45	0.34
	$x_p > 0.05$	0.64 ±0.12 ±0.21	0.68	0.53
	$x_p > 0$	0.97 ±0.18 ±0.31 [1)]	1.04	0.84
$f_o(975)$	$x_p > 0.1$	0.042±0.026±0.012	-	-
	$x_p > 0.05$	0.10 ±0.03 ±0.019	-	-
$f_2(1270)$	$x_p > 0.1$	0.11 ±0.04 ±0.03	-	0.24

[1)]Extrapolation of the results obtained for $x_p > 0.05$ to the full x_p-range, using the x_p-shape predicted by the JETSET 7.3 PS.

Figure captions

Fig.1 The raw $\pi^+\pi^-$ invariant-mass spectrum in the range $x_p > 0.1$ (open dots) and the one corrected for reflections (crosses). The solid curve is the result of the fit to expression (1). The dashed curve shows the estimate of the background. The lower part of the figure presents the corrected data after background subtraction (crosses with error bars) and a curve showing the resonance contributions from the fit.

Fig.2 The raw $K^{\pm}\pi^{\mp}$ invariant-mass spectrum in the range $x_p > 0.05$ (open dots) and the one corrected for reflections (crosses). The solid curve is the result of the fit to expression (2). The dashed curve shows the estimate of the background. The lower part of the figure presents the corrected data after background subtraction (crosses with error bars) and a curve showing the resonance contributions from the fit. The histogram shows the distribution obtained from Monte-Carlo data (see text).

Fig.3 The dependence of the (a) ρ^0 and (b) $K^*(892)$ average multiplicities per hadronic event on the centre-of-mass energy $\sqrt{s}$ in comparison with the predictions of the JETSET 7.3 PS and HERWIG 5.4. The lower-energy data are from refs.[1-9].

Fig.4 The $1/\sigma_{hadr} \cdot d\sigma/dx_p$ a) for ρ^0, $f_2(1270)$ and $f_0(975)$ (distributions for $f_2(1270)$ and $f_0(975)$ are lowered by a factor of 10 and 100 , respectively) and b) for $K^{*0}(892)$. Solid curves are predictions of the JETSET 7.3 PS for ρ^0 and $K^{*0}(892)$ and dashed curves are predictions of the HERWIG 5.4 for ρ^0, $f_2(1270)$ and $K^{*0}(892)$.

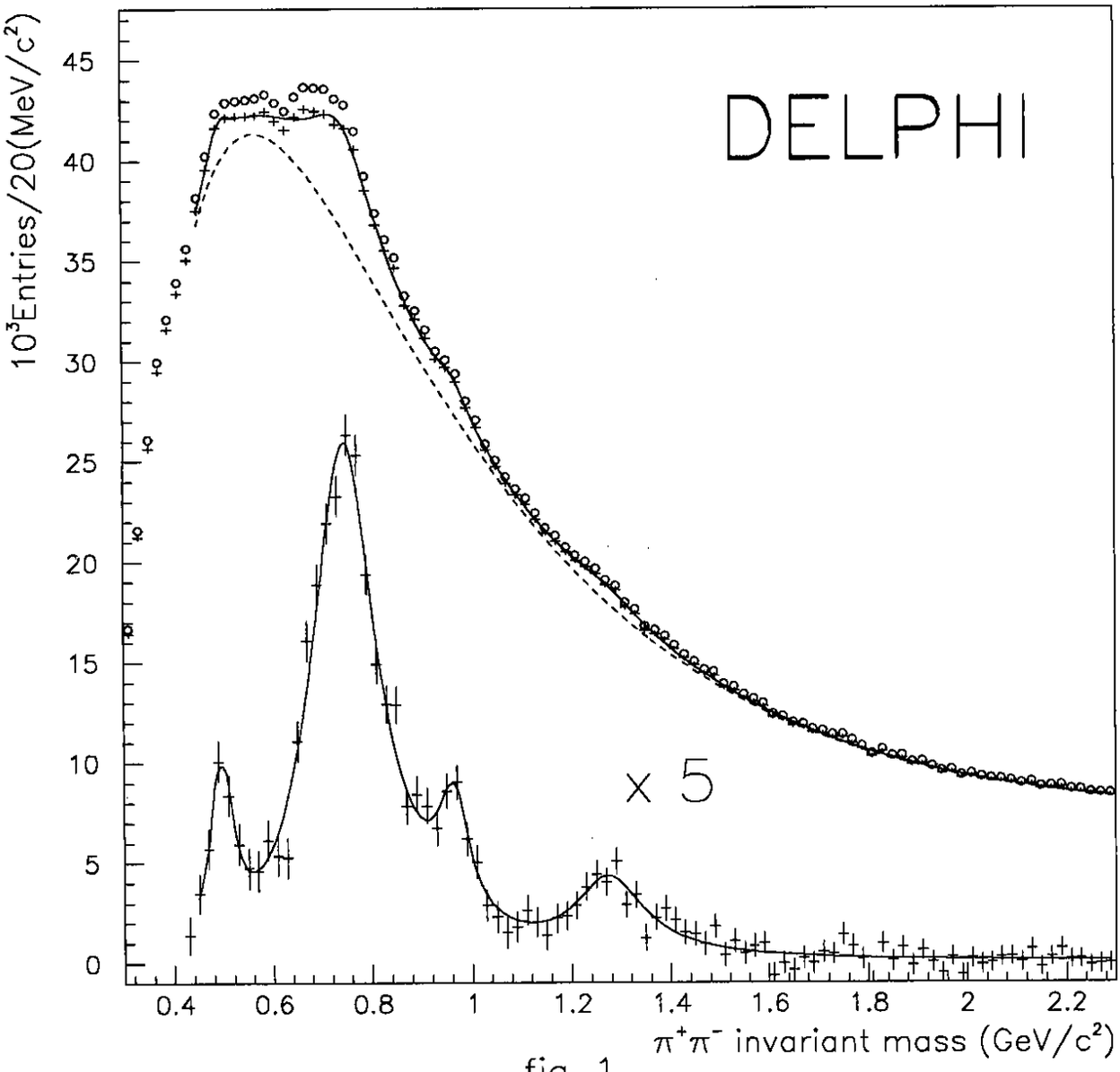
DELPHI
10^3Entries/20(MeV/c^2)
45
40
35
30
25
20
15
10
5
0
0.4
0.6
0.8
1
1.2
1.4
1.6
1.8
2
2.2
$\pi^+\pi^-$ invariant mass (GeV/c^2)
x 5

fig. 1

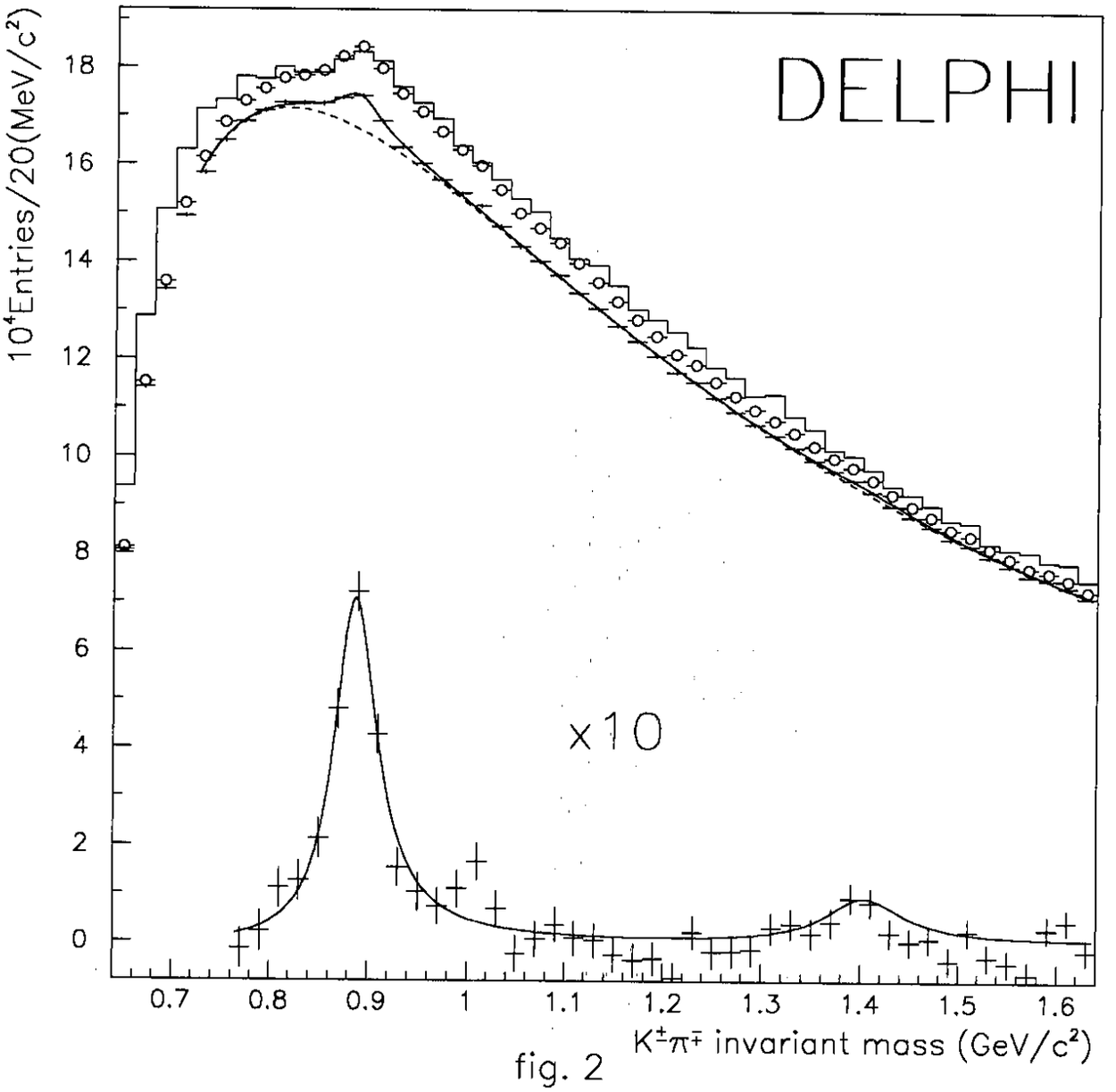
DELPHI
10^4Entries/20(MeV/c^2)
18
16
14
12
10
8
6
4
2
0
x10
0.7
0.8
0.9
1
1.1
1.2
1.3
1.4
1.5
1.6
$K^{\pm}\pi^{\mp}$ invariant mass (GeV/c^2)

fig. 2

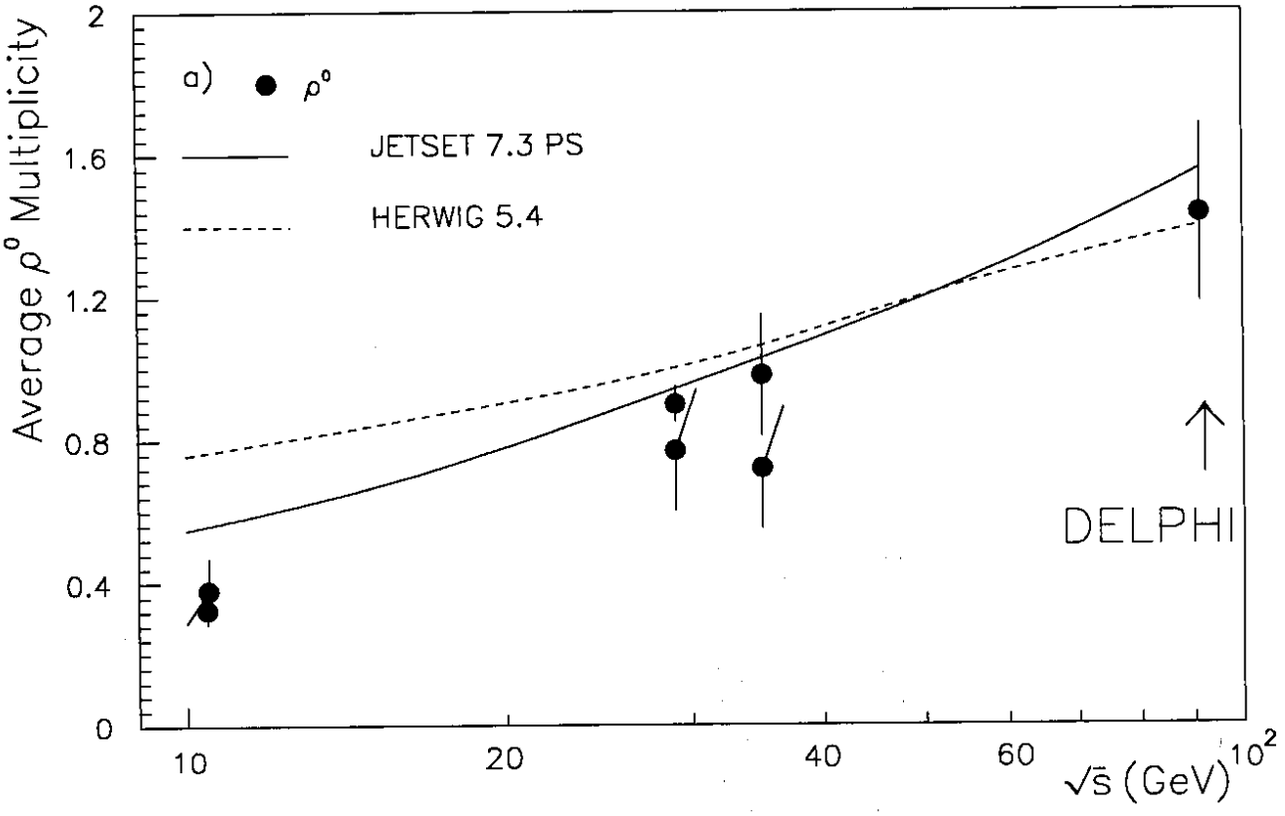
a)
ρ^0
JETSET 7.3 PS
HERWIG 5.4
DELPHI
Average ρ^0 Multiplicity
$\sqrt{s}$ (GeV)
10^2

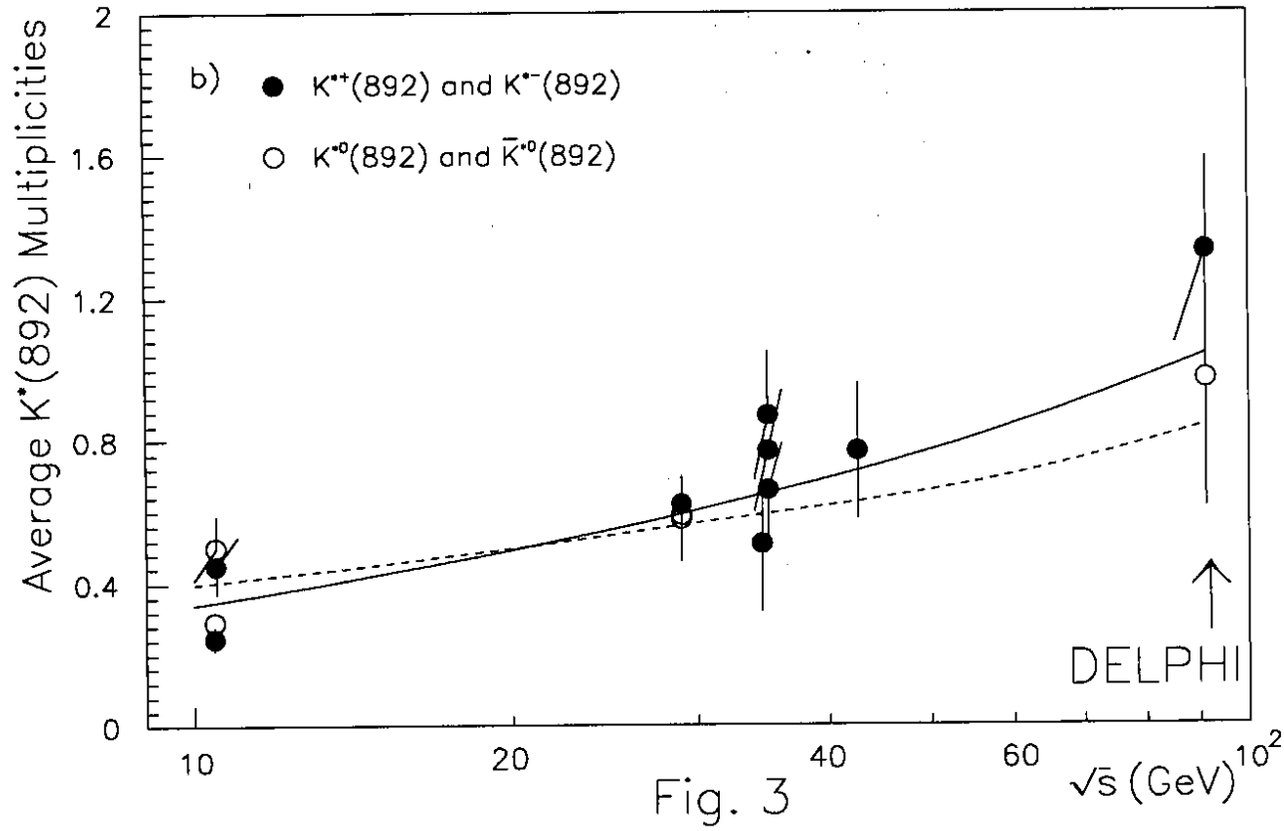
b)
$K^{*+}(892)$ and $K^{*-}(892)$
$K^{*0}(892)$ and $\bar{K}^{*0}(892)$
DELPHI
Average K*(892) Multiplicities
$\sqrt{s}$ (GeV)
10^2

Fig. 3

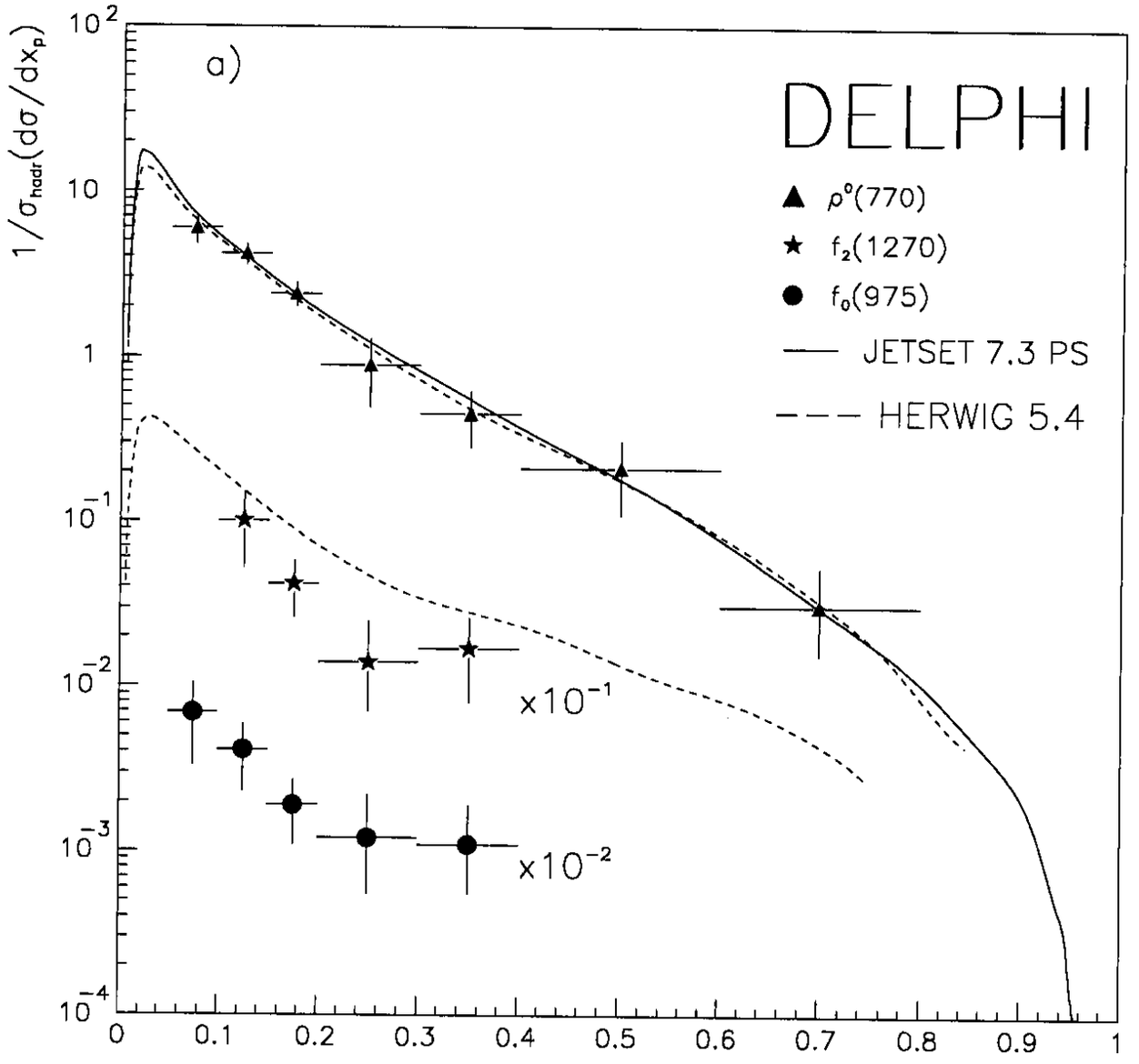
a)
DELPHI
ρ°(770)
f₂(1270)
f₀(975)
JETSET 7.3 PS
HERWIG 5.4
x10⁻¹
x10⁻²
1/σ_had(dσ/dx_p)
x_p=p/p_beam

fig. 4a

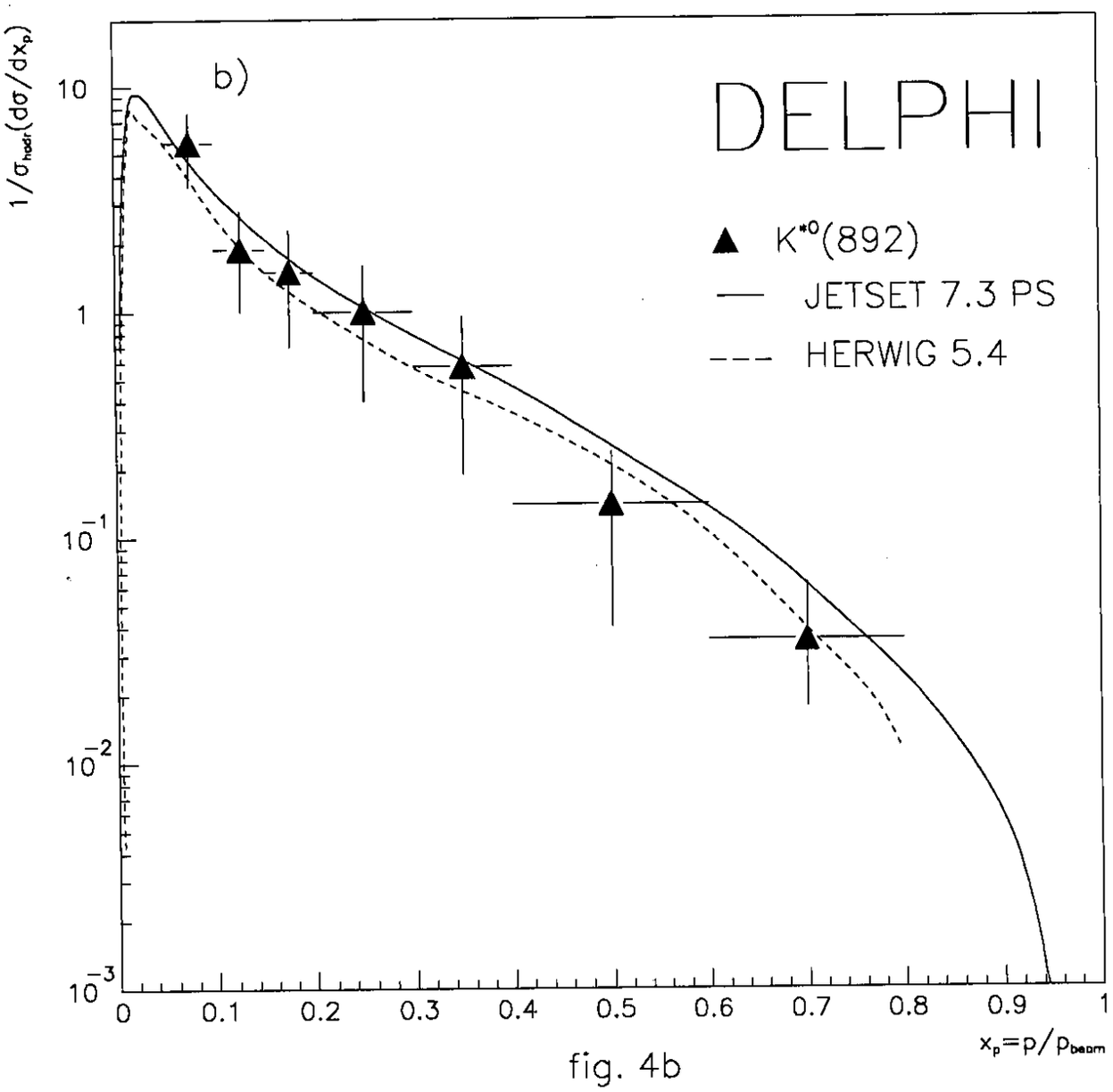
b)
DELPHI
K*0(892)
JETSET 7.3 PS
HERWIG 5.4
1/σhadr(dσ/dxp)
xp=p/pbeam
10
1
10-1
10-2
10-3
0
0.1
0.2
0.3
0.4
0.5
0.6
0.7
0.8
0.9
1

fig. 4b